ELECTRONICS AND ELECTRICAL ENGINEERING
ISSN 1392 – 1215 2010. No. 7(103)
ELEKTRONIKA IR ELEKTROTECHNIKA

ELECTRICAL ENGINEERING
T 190
ELEKTROS INŽINERIJA

A Perfectly Symmetrical Configuration in Dual-Bridge Inverter Topology for Maximum Mitigation of EMI, Common-Mode Voltages and Common-Mode Currents

H. Akroum
Département de la maintenance industrielle, Faculté des sciences de l'ingénieur,
Université M'Hamed Bougara de Boumerdès, Avenue de l'Indépendance, 35000, Boumerdès, Algeria,
phone : +213550528743, e-mail: akroum@yahoo.fr

M. Kidouche
Département d'Automatisation des Procédés et Electrification, Faculté des Hydrocarbures et de la Chimie,
Université M'Hamed Bougara de Boumerdès, 35000, Boumerdès, Algeria,
phone : +213774183083, e-mail: kidouche_m@hotmail.com

S. Grouni
Département de Physique, Faculé des Sciences,
Université M'Hamed Bougara de Boumerdès, Avenue de l'Indépendance, 35000, Boumerdès, Algeria,
phone : +213774183083, e-mail: sgrouni@yahoo.fr

M. Zelmat
Laboratoire d'Automatique Appliquée (LAA), Faculté des Hydrocarbures,
Université M'Hamed Bougara de Boumerdès, Avenue de l'Indépendance, 35000, Boumerdès, Algeria,
phone : +21324 8914, e-mail: zelmat_mimoun@yahoo.com

Introduction

The development of advanced power electronic switching devices such as insulated bipolar transistor (IGBT's) has enabled high frequency switching operation and has improved the performance of the pulse-width modulated (PWM) inverters of the adjustable speed drives (ASD's). However, the use of high frequency switching power semiconductors induces fast voltage and current variations (dv/dt and di/dt) and unavoidable parasitic capacitances witch cause the following problems:

- ground current escaping to earth through stray capacitors inside motors [1];
- bearing current and shaft voltage [2–10];
- motor over-voltage problems [11–13] and shortening of insulation life of motors and transformers [14];
- conducted and radiated electromagnetic interference (EMI) [13–25]

Common-mode voltages and common-mode currents generated by PWM frequency converters have been identified as a major cause of adverse effects in applications of PWM ASDs [3–7]. Bearing currents are the major cause of premature bearing failure in high-frequency PWM inverter-fed induction motors. The bearings are not in electrical contact with the inner and outer races because the grease used has a partial insulating effect. Therefore, the charge accumulates on the rotor assembly until it exceeds the dielectric capability of the bearing grease. The resulting effect is a frequently repeated flashover current that in time can damage the bearing surfaces due to the electric discharge machining (EDM) effect, or electroplating of the race steel and bearing ball (pitting and fluting) [3-6]. (Fig. 1) shows the advanced fluting on a bearing race [4].

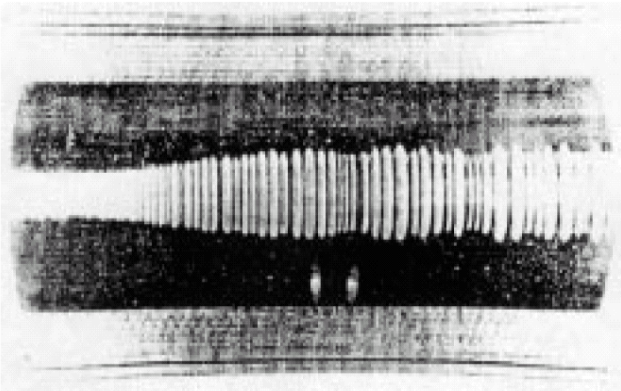

Fig. 1. Surface roughness of a ball bearing race due to electrical fluting

Step change in voltage/current produces higher electromagnetic (EM) noise mainly at the switching frequency and its harmonics. The emitted energy amplitude increases as a function of the peak current. These emissions are especially dominant in the long-wave (LW)/AM radio range [12–13]. These emissions are noticeable and can appear as distinct tones at the output of the radio [16–17].

Several mitigation techniques have been proposed to reduce the common-mode voltages and EMI generated by conventional three-phase PWM inverters. Among these techniques, the dual-bridge inverter (DBI) topology has proved to be effective in eliminating the common-mode voltage and motor bearing currents, as well as reducing the conducted EMI [7–10].

The DBI approach is based on feeding a suitably connected double-winding motor by two parallel inverter units having opposite polarities. In [10] the experimental results show that both the capacitive and induced shaft voltages are reduced by more than 80%. The remaining capacitive shaft voltage originates from the common-mode voltage generated by the rectifier. This voltage cannot be compensated by the DBI approach. The remaining induced shaft voltage is a result of non simultaneous timing of the PWM pulses of the inverter units. The common-mode current in the input cable of the converter is also effectively reduced, decreasing the conducted EMI. Simulations were carried out in [10] to investigate the effect of a time delay between the PWM pulses of the parallel inverter units. In the investigated drive, a delay as short as 15 ns caused the remaining common-mode current and induced shaft voltage.

This paper presents an improvement of the works described in [7–10]. The proposed technique employs DBI approach with a perfectly symmetrical switching configuration. The major contributions are:

- no need to additional gate drivers;
- the delay between the PWM pulses of the parallel inverter units reduced practically to less than 1ηs;
- notably reduction of radiated EMI.

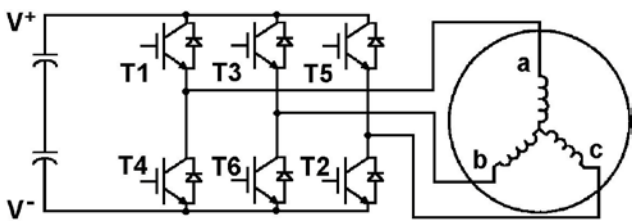

Fig. 2. Conventional PWM inverter-fed induction motor drive

Common-mode voltage generation in a three-phase PWM inverter

Conventional three-phase PWM inverters consist of three legs and six switches (Fig. 2).

The common-mode voltage is defined as

$$V_{co} = \frac{1}{3}(V_a + V_b + V_c) \ . \qquad (1)$$

When the motor is energized by a conventional PWM inverter, the resulting common-mode voltage is

$$V_{com} = \begin{cases} V^+, & \text{when T1, T3, T5 on;} \\ \frac{1}{3}V^+, & \text{when two of T1, T3, T5 on ;} \\ -\frac{1}{3}V^+, & \text{when one of T1, T3, T5 on;} \\ V^-, & \text{when T4, T6, T2 on .} \end{cases} \qquad (2)$$

Therefore the conventional inverter generates a non-zero common-mode voltage and current. In (Fig. 3), a switching pattern is shown where it can be observed how the common-mode voltage is generated. This voltage is obtained by applying the equation (1). As a consequence, a usual three-leg inverter can not have an output CM voltage equal to zero.

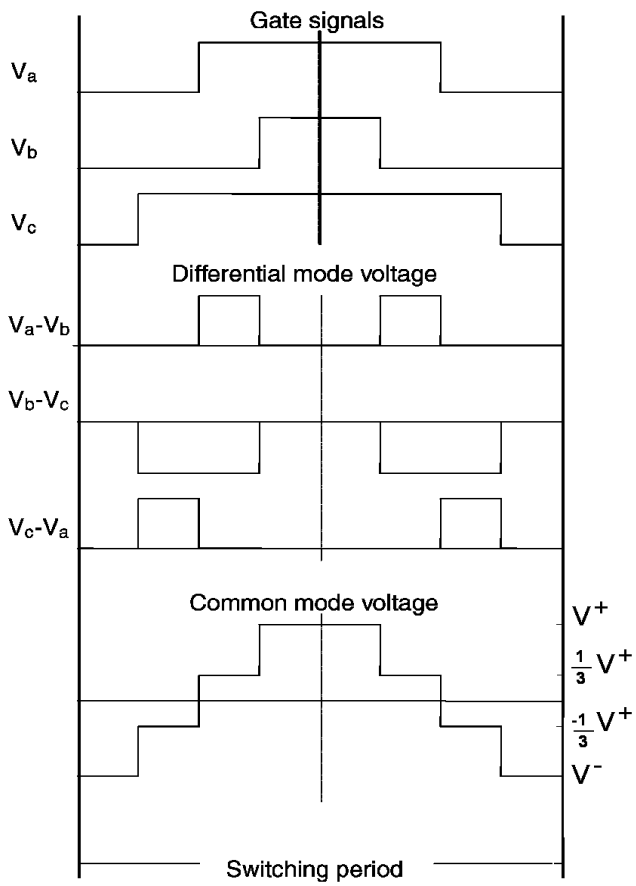

Fig. 3. Common-mode voltage generation in a PWM inverter

The dual bridge inverter approach

The prerequisites for a drive to be suitable for the DBI approach implementation are an even number of parallel inverter units in the frequency converter and an even number of parallel branches in the stator winding of the motor [7-10]. A conventional stator winding with two parallel branches is shown in (Fig. 4, a) For the DBI approach, the winding is divided into two separate three-phase windings, and the polarity of one of the windings is inverted, as shown in (Fig. 4, b) an inverter unit feeds each winding. In each switching, the corresponding phases of

the inverter units are connected to opposite DC buses, as illustrated in (Fig. 5) Thus the differential-mode voltages are equal in the corresponding branches of the two windings, but the common-mode voltages are the opposite and their sum vanishes [7-10]. The common-mode voltage is defined as:

$$V_{co} = \frac{1}{6}(V_a + V_b + V_c + V_{a'} + V_{b'} + V_{c'}) . \quad (3)$$

To eliminate the common-mode voltage V_{com} the inverter is designed and controlled such that:

$$V_{a'} = -V_a , \; V_{b'} = -V_b , \; V_{c'} = -V_c . \quad (4)$$

The output bridges and relevant switching strategy are shown in (Fig. 5) [7, 9, 10]. For example, when T_1 is on, T_4 is off and due to the reversed triggering signal to the second bridge, T_1' is off, T_4' is on, and therefore:

$$V_a + V_{a'} = 0, \; V_b + V_{b'} = 0, \; V_c + V_{c'} = 0 . \quad (5)$$

This will be the exact inverse for the condition of T_1 off and T_4 on, where $V_a = V^-$ and $V_{a'} = V^+$.

The subsequent switches will operate in a similar pattern such that in all we will have the common-mode voltage equal to zero:

$$V_{co} = \frac{1}{6}(V_a + V_b + V_c + V_{a'} + V_{b'} + V_{c'}) = 0 . \quad (6)$$

The absence of the common-mode voltage will preclude the electrostatic coupling between the rotor shaft and frame (ground). Therefore, the shaft voltage and resulting bearing current will be eliminated.

(Fig. 6, a) illustrates the common-mode current in a conventional inverter unit. (Fig. 6, b) illustrates the common-mode currents when the DBI approach is used. In the DBI approach, the common-mode currents are the opposite and their sum vanishes.

Experimental results of the dual bridge inverter approach implemented in a 1.4 MW cage induction motor drive have been described in [10]. (Table, 1) sums up the measured maximum peak values of the investigated quantities. The reduction of the peak values, obtained by using the DBI approach, is presented in the rightmost column. All relevant quantities were reduced by more than 80% [10].

Table 1. Results of conventional and DBI inverter connections (maximum peak values) [10].

	Shaft Voltage (V)		Common-mode Current (A)	
	Induced	Capacitive	Motor Cable	Input Cable
Conventional	51.5V	60V	49A	12.5A
DBI	10V	10V	7.5A	1.5A
Difference in %	−81	−83	−85	−88

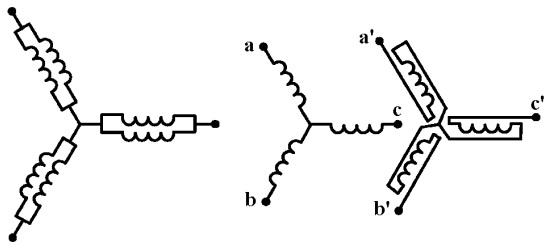

a) b)

Fig. 4. Winding arrangements: a – conventional two-branch winding; b – winding connected for DBI approach

The perfectly symmetrical switching configuration in dual-bridge inverter topology

From (Fig. 5) it is clear that (T_1, T_4') have the same triggering signal, in consequence the gates of (T_1, T_4') can be connected together. The same remark can be observed for (T_2, T_5'), (T_3, T_6'), (T_4, T_1'), (T_5, T_2') and (T_6, T_3'). The perfectly symmetrical switching configuration in the DBI topology, shown in (Fig. 7), takes advantage of these remarks. With this configuration (Fig. 7), no need for additional gate drivers and the time delay between the PWM pulses of the parallel inverter units can be reduced practically to less than 1ηs. The DBI topology has proved, by simulation and experimental validation, in [7-10], to be effective in eliminating the CM voltage and motor bearings currents, as well as reducing the conducted EMI. However, the radiated EMI in DBI approach has not been discussed. With the configuration of (Fig. 7) notably reduction of radiated EMI can be obtained.

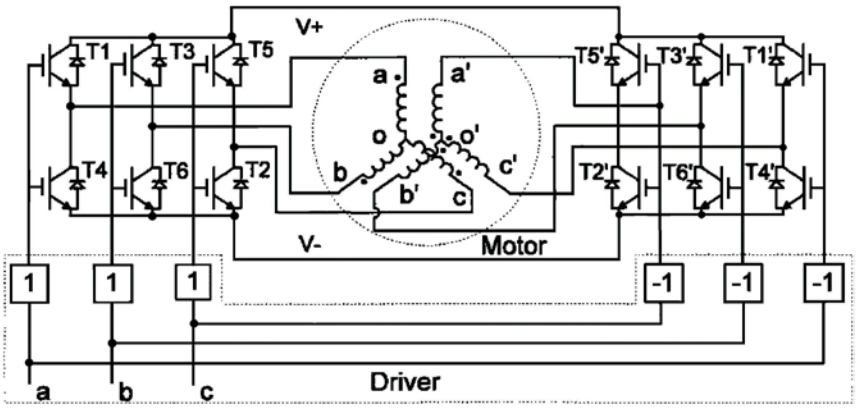

Fig. 5. Proposed PWM dual-bridge inverter drive in [7, 10]

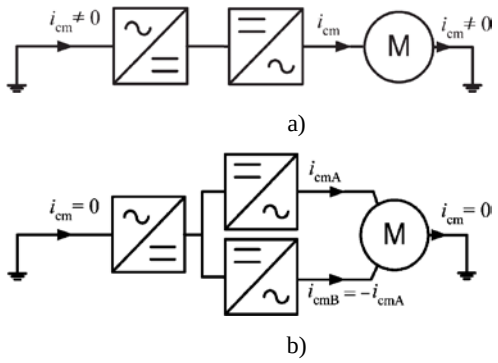

Fig. 6. Common-mode current paths: a – conventional inverter; b – DBI approach ($I_{cmB} = -i_{cmA}$)

Verification by simulation

In this section, the verification by simulation of the effective reduction of radiated EMI in DBI approach using the perfectly symmetrical switching configuration is presented. For this purpose equivalent loop antennas have been used [26, 27].

As shown in (Fig. 8, a), two circular-loop antennas positioned symmetrically on the x-y plane, respectively, at z=0 and z=d. The wire is assumed to be very thin, the radius of the loop a<<λ, λ the wavelength, and the current I is taken constant along the loops.

For the circular loop antenna of (Fig. 8, b), in near field region (kr<<1, with k=2π/λ), the magnetic field component can be expressed as [26, 27]:

$$H_\theta \approx \frac{a^2 I e^{-jkr}}{4r^3} \sin\theta\,, \tag{7}$$

$$H_r \approx \frac{a^2 I e^{-jkr}}{2r^3} \cos\theta\,, \tag{8}$$

$$H_\varphi = 0\,. \tag{9}$$

Thus the amplitude of the magnetic field is

$$H \approx \frac{a^2 I}{2r^3}\sqrt{\frac{3\cos(2\theta)+5}{8}}\,, \tag{10}$$

The field radiated by the two loops (Fig. 8, a) was investigated by means of computer simulations. In the simulation the distance d between the loops was varied and the magnetic field reduction in % was observed.

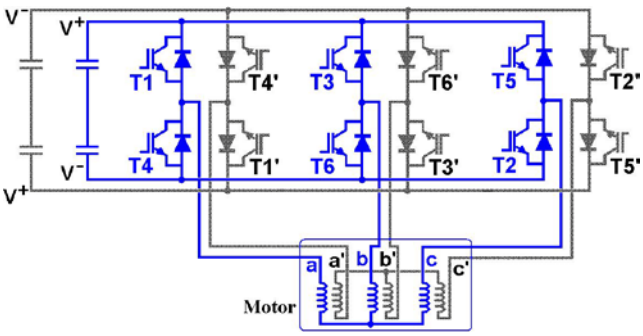

Fig. 7. Proposed perfectly symmetrical switching configuration in the DBI topology

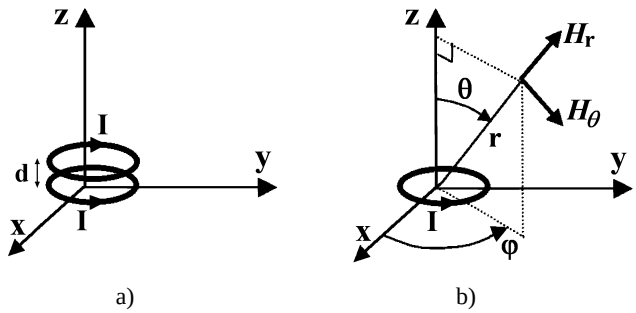

Fig. 8. Geometrical arrangement for the circular-loop antennas

Simulated magnetic field reduction as a function of the distance between the two loops is shown in (Fig. 9). The field was observed at (z=1m, y=0m, x=-0.2 to 0.2m). It was found that a distance between the loops less than 5cm can reduce the radiated field by more than 90%.

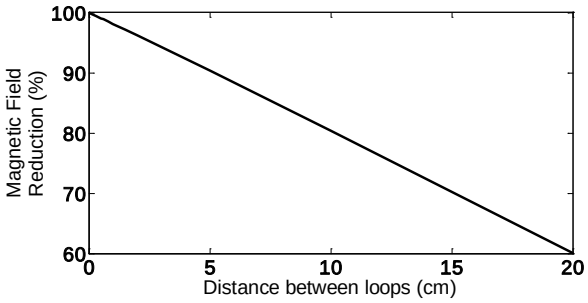

Fig. 9. Simulated magnetic field reduction (in %) as a function of the distance between the two loops (in cm)

Conclusions

In this paper, we presented an improvement of the DBI approach. The proposed technique employs DBI topology with a perfectly symmetrical switching configuration. The major contributions were:

- no need to additional gate drivers;
- the delay between the PWM pulses of the parallel inverter units reduced practically to less than 1ηs;
- notably reduction of radiated EMI.

Verification by simulation of the effective reduction of radiated EMI in DBI approach using the perfectly symmetrical switching configuration was presented. The near field radiated by two circular current loops was investigated by means of computer simulations. A notably reduction of radiated EMI was verified.

References

1. **Murai Y., Kubota T., Kawase Y.** Leakage current reduction for a high–frequency carrier inverter feeding an induction motor // IEEE Transactions on Industry Applications. – 1992. – Vol. 28. – P. 858–863.
2. **Chen S., Lipo T. A., Fitzgerald D.** Source of induction motor bearing currents caused by PWM inverters // IEEE Transactions on Energy Conversion. – 1996. – Vol. 11. – P. 25–32.
3. **Chen S., Lipo T. A, Fitzgerald.** Modeling of motor bearing currents in PWM inverter drives // IEEE Transaction on Industry Applications. – 1996. – Vol. 32. – P. 1365–1370.

4. **Busse D., Erdman J., Kerkman R., Schlegel D., Skibinski G.** Characteristics of shaft voltage and bearing currents // IEEE Industry Application Magazine. – 1997. – P.21–32.
5. **Chen S., Lipo T. A**. Bearing currents and shaft voltages of an induction motor under hard and soft–switching excitation // IEEE Transactions on Industry Applications. – 1998. –Vol. 34. – P. 1042–1048.
6. **Chen S., Lipo T. A.** Circulating type motor bearing current in inverter drives // IEEE Industry Application Magazine. – 1998. – P. 32–38.
7. **Von Jouanne A., Zhang H.** A dual–bridge inverter approach to eliminating common–mode voltages and bearing and leakage currents // IEEE Transactions on Power Electronics. – 1999. – Vol. 14. – P. 43–48.
8. **Zhang H., Von Jouanne A., Dai S.** A Reduced–Switch Dual–Bridge Inverter Topology for the Mitigation of Bearing Currents, EMI, and DC–Link Voltage Variations // IEEE Transactions on Industry Applications. – 2001. – Vol. 37. – No. 5. – P. 1365–1372.
9. **Zhang H., Von Jouanne A.** Suppressing common–mode conducted EMI generated by PWM drive systems using a dual–bridge inverter // Proceedings of the applied power electronics conference and exposition, Anaheim (APEC ’98). – 1998. – P.1017–1020
10. **Mäki–Ontto P., Luomi J., Kinnunen H.** Reduction of capacitive and induced shaft voltages in an induction motor drive using dual–bridge inverter approach // Electrical Engineering. – 2006. – Vol. 88. – P. 465–472.
11. **Gacek Z. Skomudek, W.** Influence of Selected Parameters of Overvoltages on Hazard of Insulating Systems in MV Power Lines // Electronics and Electrical Engineering. – Kaunas: Technologija, 2006. – No. 2(66). – P. 88–91.
12. **Kepalas V. P., Ramonas C. S.** Overvoltages in the Asynchronous PWR Converter Cascade Drive // Electronics and Electrical Engineering. – Kaunas: Technologija, 1999. – No. 3(21). – P. 24–28.
13. **Moreira A. F., Santos P. M., Lipo T. A., Venkataramanan G.** Filter Networks for Long Cable Drives and Their Influence on Motor Voltage Distribution and Common–Mode Currents // IEEE Transactions on Industrial Electronics. – 2005. –Vol. 52. – No. 2. – P. 515–522.
14. **Bose B. K.** Power electronics and motor Drives recent progress and perspective // IEEE Transactions on Industrial Electronics. – February, 2009. – Vol. 56. – P. 581–588.
15. **Knurek D. F.** Reducing EMI in switch mode power supplies // 10th International Telecommunications Energy Conference (INTELEC'88). – 1988. – P. 411–420.
16. **Jabbar M. A., Rahman M. A.** Radio frequency interference of electric motor and associated controls // IEEE Transactions on Industry Applications. – 1991. – Vol. 27. – P 27–31.
17. **Zhong E., Chen S., Lipo T. A.** Improvements in EM1 Performance of Inverter–Fed Motor Drives // Applied Power Electronics Conference and Exposition (APEC'94). – 1994. – Vol. 2. – P. 608–614.
18. **Ogasawara S., Akagi H.** Modeling and damping of high–frequency leakage currents in PWM inverter–fed AC motor drive systems // IEEE Transactions on Industry Applications. – 1996. – Vol. 32. – P. 1105–1113.
19. **Ogasawara S., Ayano H., Akagi H.** Measurement and reduction of EMI radiated by a PWM inverter–fed AC motor drive system // IEEE Transactions on Industry Applications. – 1997. – Vol. 33. – No. 4. – P. 1019–1926.
20. **Mutoh N., Nakashima J., Kanesaki M.** Multilayer Power Printed Structures Suitable for Controlling EMI Noises Generated in Power Converters // IEEE Transactions on Industrial Electronics. – 2003. – Vol. 50. – No. 6. – P. 1085–1094.
21. **Akagi H., Doumoto T.** A Passive EMI Filter for Preventing High–Frequency Leakage Current From Flowing Through the Grounded Inverter Heat Sink of an Adjustable–Speed Motor Drive System // IEEE Transactions on Industry Applications. – 2005. – Vol. 41. – P. 1215–1223.
22. **Fardoun A. A., Comstock L., Rakouth H.** Reduction of EMI Through Switching Dithering // Delphi Technologies Inc. – 2004. – U.S. Patent 6 674 789 B1.
23. **Fardoun A. A., Ismail E. H.** Reduction of EMI in AC Drives Through Dithering Within Limited Switching Frequency Range // IEEE Transactions on Power Electronics. – 2009. – Vol. 24. – No. 3. –P. 804–811.
24. **Wang Z., Chau K. T., Liu C.** Improvement of Electromagnetic Compatibility of Motor Drives Using Chaotic PWM // IEEE Transactions on Magnetics. – 2007. – Vol. 43. – No. 6. – P.2612–2614.
25. **Zumel P., Garcia O., Oliver J. A, Cobos J. A.** Differential–Mode EMI Reduction in a Multiphase DCM Flyback Converter // IEEE Transactions on Power Electronics. – August 2009. –Vol. 24. – No. 8. –P. 2013–2020.
26. **Balanis C. A.** Antenna Theory, Analysis and Design (3rd ed.). – John Wiley & Sons, New Jersey, 2005. –1118 p.
27. **Perez R.** Wireless communications design handbook: aspects of noise, interference, and environmental concerns, V.3. Interference into circuits. – USA: Academic Press, CA, 1998. – 458 p.

Submitted 2010 02 14

H. Akroum, M. Kidouche, S. Grouni, M. Zelmat. A Perfectly Symmetrical Configuration in Dual-Bridge Inverter Topology for Maximum Mitigation of EMI, Common-Mode Voltages and Common-Mode Currents // Electronics and Electrical Engineering. – Kaunas: Technologija, 2010. – No. 7(103). – P. 51–56.

This paper presents a new idea for the mitigation of EMI, Common-Mode Voltages and Common-Mode Currents in an Induction Motor Drive. The proposed technique employs dual bridge inverter approach with a perfectly symmetrical switching configuration. The major contributions are: no need to additional gate drivers, the delay between the PWM pulses of the parallel inverter units reduced practically to less than 1ηs, and notably reduction of radiated EMI. Verification by simulation of the effective reduction of radiated EMI in DBI approach using the perfectly symmetrical switching configuration is presented. Ill. 9, bibl. 27, tabl. 1 (in English; abstracts in English, Russian and Lithuanian).

Х. Акроум, М. Кидоуше, С. Гроуни, Н. Зелмат. Исследование метода уменьшения напряжения и тока в двухмостовом симметричном инверторе // Электроника и электротехника. – Каунас: Технология, 2010. – № 7(103). – С. 51–56.

Описываются способы уменьшения тока в асинхронном двигателе. Созданный новый метод основан на применении двухмостовых симметричных инверторов. Предложенный вариант проверен методом моделирования. Ил. 9, библ. 27, табл. 1 (на английском языке; рефераты на английском, русском и литовском яз.).

H. Akroum, M. Kidouche, S. Grouni, M. Zelmat. EMI srovių, bendrųjų įtampų ir srovių mažinimo dvitilčiame simetriniame inverteryje tyrimas // Elektronika ir elektrotechnika. – Kaunas: Technologija, 2010. – Nr. 7(103). – P. 51–56.

Pasiūlytas naujas metodas asinchroninio variklio EMI srovėms, bendrosioms įtampoms ir srovėms mažinti. Jis pritaikytas dvitilčiame simetriniame inverteryje. Tokiu atveju nereikia papildomo užtvarinio variklio, impulsinės platuminės moduliacijos impulsų tarpusavio vėlinimas sumžinamas iki 1 ηs ir ypač sumažinama EPI spinduliuotė. Metodas patikrintas modeliuojant. Il. 9, bibl. 27, lent. 1 (anglų kalba; santraukos anglų, rusų ir lietuvių k.).